Journal of Minerals and Materials Characterization and Engineering, 2025, 13(1), 1-17
https://www.scirp.org/journal/jmmce
ISSN Online: 2327-4085
ISSN Print: 2327-4077

Preparation and Characterization of Clay Soils for Applications in Cyanide Removal from Mining Wastewater

Raymond Kaboré[1], Yacouba Sanou[1*], Rasmane Tiendrebéogo[1], Alassane Compaoré[2,3], Adama Konaté[4], Samuel Paré[1]

[1]Chemistry Department, University Joseph Ki-Zerbo, Ouagadougou, Burkina Faso
[2]Department of Physics, Kenyatta University, Nairobi, Kenya
[3]Department of Civil Engineering, Worcester Polytechnic Institute, Worcester, USA
[4]Physic Department, University Joseph Ki-Zerbo, Ouagadougou, Burkina Faso
Email: *prosperyacson@gmail.com

How to cite this paper: Kaboré, R., Sanou, Y., Tiendrebéogo, R., Compaoré, A., Konaté, A. and Paré, S. (2025) Preparation and Characterization of Clay Soils for Applications in Cyanide Removal from Mining Wastewater. *Journal of Minerals and Materials Characterization and Engineering*, **13**, 1-17.
https://doi.org/10.4236/jmmce.2025.131001

Received: October 17, 2024
Accepted: December 24, 2024
Published: December 27, 2024

Abstract

In Burkina Faso, water resources in mining areas are polluted by cyanide, which is released into the environment through mining activities. To mitigate this pollution, two clays named Koro and Kaya were collected in Burkina Faso and characterized using analytical technics. This work aimed to find out a cheap technology based on local soils for water treatment. The objective of the work was to prepare and characterize two local clays for application in mining effluent treatment. Specific surface area and pore dimensions were analyzed using Brunauer, Emmett and Teller method. In addition, anion exchange capacities, chemical composition through X-ray fluorescence and chemical functions by Fourier-transformed Infrared spectroscopy were determined. Mineralogical composition, thermal behavior, microstructure, and surface elemental composition of clays were examined using techniques of X-ray diffraction and scanning electron microscopy coupled with energy dispersive spectroscopy. Results showed that the surface areas of two anionic clays were 64 m^2/g and 50 m^2/g for Koro and Kaya, respectively. An anion exchange capacity of 126.68 cmol/kg for Koro and 125.13 cmol/kg at pH 11 was found. Chemical and mineralogical analysis showed that the clays were rich in minerals, mainly of illite (24 - 27)%, montmorillonite (23 - 24)% and kaolinite (17 - 26)%, orthosis (9 - 13)%, quartz (5 - 12)%, goethite (3 - 6)% and anorthite (2 - 6)%. Application of clays for the treatment of cyanide solution led to a decrease in intensities of chemical functions and a modification of the surface morphology. Consequently, those clay soils can be used as adsorbents in cyanide removal through column and batch experiments.

Keywords

Clays, Chemical Properties, Mineralogical Compostion, Cyanide, Metal-Cyanide Complex, Wastewater

1. Introduction

In Burkina Faso, gold is the main resource exploited with a significant use of cyanide or mercury for ores processing [1]. The uncontrolled discharge of wastes from there in the environment has led to the contamination of surface and groundwater by cyanide in mining areas [2] [3]. Cyanide is toxic to all living organisms [4]. The toxicity of cyanide comes from the fact that it has an affinity to complex itself to all metals, leading to an inhibition of enzymes whose active centers are iron, copper, and cobalt [5]. They block the respiration of the cells that transport oxygen from the blood to the tissues [6]. Cyanide can be removed from water by adsorption on synthetic or natural adsorbents [7]. The most commonly used synthetic adsorbents in cyanide adsorption are activated carbons [8] [9]. Mbadcam *et al.* [7] successfully used activated carbon at pH 10.8 - 11 for cyanide removal. Manyuchi *et al.* [10] used biochar for cyanide removal in wastewater at pH 7 and found a reduction of 75%. However, activated carbon production is energy-intensive and produces a large quantity of carbon dioxide, which is a greenhouse gas. Another way to remove cyanide is the chemical oxidation using peroxide, chloride and ozone to transform cyanide into cyanate form. This produces hazardous materials that need further treatment. For instance, the conversion of cyanogen chloride to cyanate is highly limited at pH values lower than 8. Chlorination, however, has a number of drawbacks at high pH levels, including the need for large amounts of chlorine in situations of high concentration and thiocyanate present, poor cyanide complex removal, and significant generation of heavy metal-containing sludge that needs additional treatment [11]. Ozonation is less effective at pH levels where cyanide stability exists, but it is extremely damaging toward thiocyanates and WAD cyanide [12]. The research of eco-friendly adsorbents, available and accessible at a lower cost in Burkina Faso, led to the use of clays in the removal of pollutant from wastewater. In fact, clays are hydrated phyllosilicates made up of fine fractions of rocks, sediment and soils. Depending on the rock's source and climate, they are made up of different minerals such as illite, kaolinite, smectite, anorthite, montmorillonite, materials that are amorphous to X-rays, such as organic raw material, allophane and imogolite often called associated phases. Clay minerals can be synthetic, unlike clay [13] [14]. They have enormous potential for various industrial applications. In addition to their conventional uses as ceramic materials (porcelain, bricks), clays are used in many industrial processes, such as papermaking, cement production, in the oil industry as drilling muds; catalysts in refining, in the treatment of vegetable and mineral oils as bleaching agents [15]. In environment, clays act as natural scavengers of pollutants by absorbing cations

and anions. Clays are used as filters for the removal of debris, dirt and microbes or bacteria from the wastewater [16]. In Burkina Faso, studies using clay materials showed a better potential in the treatment of tannery wastewater for chromium removal [17] and drilling water for the removal of lead, copper and chromium [18].

Their adsorbent properties vary according to chemical and mineralogical compositions, but the factors that control these properties are not well understood. The best-known properties are their large specific surfaces due to their small sizes, sheet shapes, charged networks and cation and anion exchange capacities [19]. In order to have a material optimally exploited as an adsorbent, its various chemical, physical and mineralogical properties must be known. The objective of this work was to characterize two clay raw materials for cyanide removal. The physical, chemical, thermal and mineralogical properties that may impact adsorption efficiency were determined.

2. Materials and Methods

2.1. Preparation of Clays Materials

The clay called Koro was collected in Koro clay site (11.15˚N, 04.18˚W), located at 15 km from Bobo Dioulasso city. The second clay named Kaya was collected at Roumbila site (13.07887˚N; 0.7842˚W) located 36 km from Kaya as indicated in Figure 1. During the sampling, Clays are taken from a depth of at least 30 cm from the surface to avoid surface contamination. Both clay quarries are exploited by potters for the manufacture of ceramic objects and for the construction of dwelling houses. The raw clay soils were crushed in particles, washed several times with distilled water to remove waste, and dried at 105˚C. Samples were crushed and immersed in distilled water for wet sieving to collect the finest fractions ≤ 2 µm. The fine fractions obtained in paste-like forms are dried at 105˚C and sieved mechanically with sieves of diameter 100; 90; 80 and 63 µm. Fractions of dimensions less than 63 µm were used for the characterization.

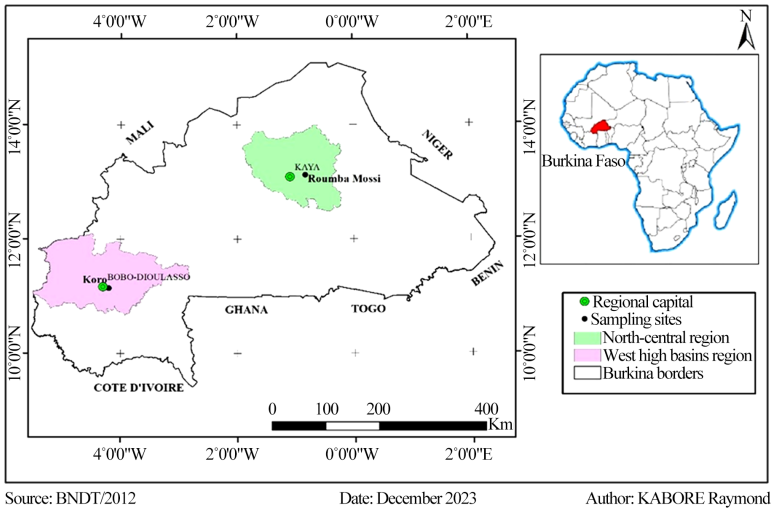

Figure 1. Identification of location of clays sampling sites on Burkina Faso's map.

2.2. Characterization of Clays

2.2.1. Moisture Content

Measurement of moisture content (H) was carried out using the method proposed by Callaud *et al.* [20]. It consisted of determining the mass of water removed by drying a wet material until a constant mass is obtained at a temperature of 105˚C ± 5˚C. The mass of material after drying is considered as the mass of solid particles (m_s). The determination of moisture content was calculated from the ratio of the mass of water (m_{water}) to the mass of solid particles (m_s).

$$H = (m_{water}/m_s) * 100 = \frac{(m_t - m_s)}{m_s} * 100 \quad (1)$$

m_{water}: water mass (g).

m_s: dry sample mass (g).

m_t: wet sample mass.

2.2.2. Specific Surface Area

Specific surface area of clays was determined using Brunauer, Emet and Teller (BET) method that consists of determining adsorption isotherm of nitrogen gas at a temperature very close to its boiling point (77˚K).

Specific surface area can be obtained from equation [21]:

$$S_{BET} = \frac{V_M * N_a * \sigma}{22,414} \quad (2)$$

S_{BET} : total area of sample (m^2/g).

N_a : Avogadro's number ($6,0224 \times 10^{-23}$ mol^{-1}).

σ : area occupied by an adsorbate molecule at 77˚K (m^2).

V_M : volume of vapor required to completely coat surface of solid with a molecular monolayer of the adsorbate (L).

2.2.3. Anion Exchange Capacity

Fixing an anion that can bind in an indiscriminate manner, like Cl^- or NO_3^-, and replacing it with another anion of the same ionic strength is known as Anion Exchange Capacity (AEC).

The method of AEC determination is the one developed from previous studies [22]. Experimentally, 1 g of clay was introduced into a 50 ml centrifuge tube previously dried and weighed, containing 25 ml of a 0.1 M NH_4Cl solution used to saturate the sites. The tube was manually agitated for 30 minutes and then left to rest for 24 h then centrifugation at 2000 rpm is done for 10 minutes and clear solution carefully siphoned. Residual chloride ions concentration was quantified and denoted as C_1. The residue is stirred again with 50 ml of a 0.001 M NH_4Cl solution for 30 minutes for washing and then left to rest for 24 hours. The concentration of chloride ions is denoted C_2. Chloride ion content is measured in both solutions to quantify portion retained per gram of dry clay. Chloride ions are replaced by nitrate ions (NO_3^-) by introducing 50 ml of a molar solution of sodium nitrate. Mixture is stirred for 30 minutes and then left to rest for 24 hours, the supernatant is siphoned off, the chloride ion content quantified and noted as C3.

$$t_1 = \frac{(0.1*0.025+0.001*0.05)-\left[C_1*(0.025-V_1)+C_2*(0.05+V_1)\right]}{m} \quad (3)$$

$$t_2 = \frac{C_3*(0.05+V_2)-C_2*V_2}{m} \quad (4)$$

$$AEC\left(\frac{mol(-)}{kg}\right)=t_1-t_2 \quad (5)$$

m: clay mass (kg).

V_1: *volume of NaCl of concentration C_1 trapped in the clay*.

V_2: volume of NaCl of concentration C_2 trapped in the clay.

t_1: content of the retained charges (−) per kilogram of clay.

t_2: content of negative charges (−) exchanged.

2.2.4. Chemical Characterization

Soils were analyzed by Energy Dispersive X-Ray Fluorescence (EDXRF). Samples were irradiated by X-rays generated by a 109 Cd ring source; the angle of incidence was 49.76˚. The detection of the characteristic X-ray radiation of the sample was performed with a Si (Li) detector (Canberra) cooled with liquid nitrogen with the following characteristics: detector size 30 mm^2, thickness 3mm. Be window = 25 μm, FWHM for 5.9 keV 55 Fe 165 eV. The emergent angle was 74.05˚ and the distance was 1.5 cm. Spectra were collected by the Genie-2000 software (Canberra, Meriden, CT United States). Infrared (IR) spectroscopy relies on the absorption of light by most molecules within a wavelength interval by converting the adsorbed intensity into molecular vibration. This absorption corresponds specifically to the bonds present in molecule. It is a non-destructive method for determining surface chemical functions and predicting likely interactions with pollutants. Infrared spectra of this clays were recorded in the mid-infrared (400 - 4000 cm^{-1}) where the fundamental vibration modes appear through a Shimadzu spectrometer equipped with FTIR ATR [14]. For structural morphology and surface chemical composition determination, clays are analyzed using a Scanning Electron Microscopy coupled with Energy Dispersive Spectroscopy (SEM-EDS, Microspec-WDX 600/OXFORD).

Thermogravimetry is a technique based on sample mass variation as a function of speed of heating. The thermal behavior of clays was determined using the TGA/DTG method. Approximately 10 mg of the sample was weighed into a ceramic crucible and placed in a thermogravimetric analyzer (NETZSCH 209 F1 Libra, Exton, Pennsylvania, USA). The samples were then heated at a rate of 10˚C per minute between 30˚C and 600˚C.

2.2.5. Mineralogical Analysis

Clays with dimensions of less than 63 μm are compacted on a glass slide in order to have a flat surface. X-ray diffractogram recordings were made by Rigaku Miniflex 6G PXRD diffractometer, with pitch of 0.05˚, a speed of 1.5˚/min and an angle of two theta between 5˚ and 65˚. From the analysis of X-ray diffraction and chemical composition, the semi-quantitative analysis of the different mineral

phases has been carried out according to methods described in literatures [23] [24].

Based on the following approximations, Equation (6) makes it possible to determine proportions of minerals in the different clays:

- Potassium oxide comes from illite;
- Calcium oxide comes only from anorthite;
- Iron oxide comes from goethite and hematite.

$$T(a) = \sum M_i * P_i(a) \tag{6}$$

$T(a)$: oxide "a" content in sample.

M_i: mineral "i" percentage in sample.

$P_i(a)$: oxide "a" proportion in mineral "i" (this proportion is deduced from ideal formula assigned to the mineral "i").

3. Results and Discussion

3.1. Physical Characteristics

At physical appearance, Kaya and Koro clays were respectively whitish and brown in color (**Figure 2**), which could highlight that is rich in alumina and Koro in iron oxide and or anorthite. Previous works showed that the pH at the zero point charge (pH_{ZPC}) was 8.22 and 7.98 for Koro and Kaya, respectively [25]. All physical properties of clays are listed in **Table 1**. It was observed a high anionic exchange capacity of two clays (126.68 cmol/kg for Koro and 125.13 cmol/kg for Kaya). Anionic clays have a sheet structure that is very favorable to anionic exchange properties, trapping of organic molecules or anions such as CN^-. Bulk densities were relatively low compared to that reported Elsewhere [26], which could reflect a low heavy metal content. The Loss on Ignition (LOI) was 8.36% and 7.21% for Koro and Kaya clays, respectively. These clays have more or less the same bound water content and/or hydroxide functions.

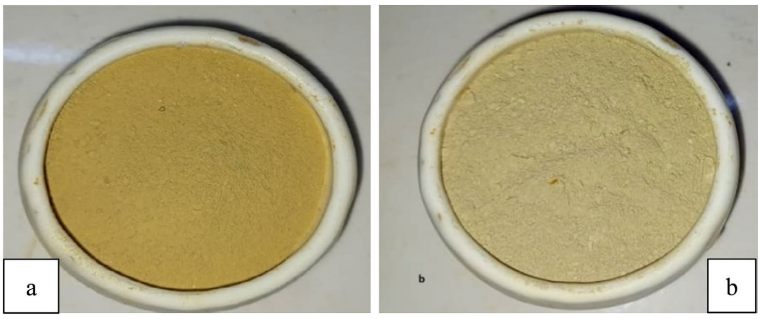

Figure 2. Images of crushed cays: (a) Koro; (b) Kaya.

Table 1. Physicochemical characteristics of Koro and Kaya.

	pH_{ZPC}	Bulk density	H (%)	LOI (%)	Color	AEC (cmol/kg)
Koro	8.22	1.27	4.83	8.36	Brown	126.68
Kaya	7.98	1.24	22.5	7.21	Whitish	125.13

Figure 3 shows that nitrogen adsorption isotherms on these clays are of type IV, characteristic of mesoporous materials [27]. In Figure 4, Koro curve was bi-modal [28], showing a pore concentration of 16.5 nm and 35.4 nm in diameter, different particles size. The pore distribution of Kaya clay was homogeneous, more than 85% of pores are less than 50 nm in diameter with more particles of same size. The values of the specific BET surfaces (Table 2) are respectively 36.21m^2/g and 21.72 m^2/g for the Koro and Kaya clays. Comparing these numbers to those reported in [29], they are deemed large. Langmuir's surface value was larger for Koro (46.55 m^2/g) comparatively to Kaya (27.33 m^2/g), showing a more favored physisorption. Because of the chosen particle size, the two clays have the same porosity volume. Internal specific surface area of the micropores was 33.37 m^2/g and 22.17 m^2/g respectively for Koro and Kaya. The significant mesopore content in the Kaya clay is confirmed by the specific exterior surfaces of the Koro and Kaya clays, which are 30.76 and 27.83 m^2/g, respectively. Smectite and vermiculite may be present in trace amounts or absent entirely in Koro and Kaya clays, which can be identified by comparing their particular surfaces to those of clay minerals [30]. These clays are thought to be composed of kaolinite, montmorillonite and illite.

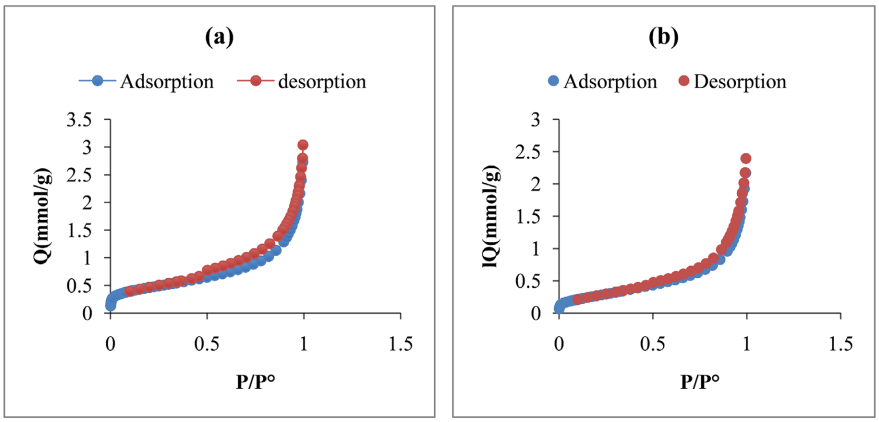

Figure 3. Adsorption and desorption isotherm of nitrogen onto (a) Koro and (b) Kaya.

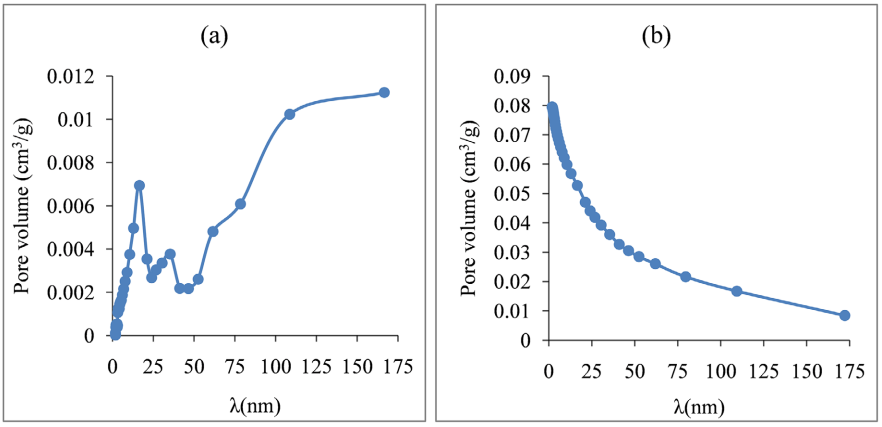

Figure 4. Pore size distribution of (a) Koro and (b) Kaya.

Table 2. Surface areas and pore dimensions of clays.

	Ss BET (m^2/g)	Langmuir Ss (m^2/g)	Pore volume (cm^3/g)	Pore radius (µm)	Internal Ss (m^2/g)	External Ss (m^2/g)	Total Ss (m^2/g)
Koro	36.206	46.546	0.058	0.611	33.369	30.760	64.129
Kaya	21.716	27.325	0.067	0.745	22.165	27.834	50.000

Ss: Specific surface.

From thermal analysis (Figure 5), two endothermic peaks were observed on the DTG curves of each clay. The first peak between 30˚C and 100˚C, with a mass loss of 4.05% for Koro and between 30˚C to 150˚C, with a mass loss of 3.05% for Kaya could be linked to the evaporation of water or carbonization of organic matters. The second peak between 400˚C and 500˚C on both clay thermograms with mass losses of 1.6% and 1.8% respectively for Koro and Kaya, are related to silicate dehydroxylation or quartz transformation. According to previous study [31], the following temperature ranges can be assigned: water bound to cations (0˚C - 250˚C), hydroxides (250˚C - 400˚C), silicates (400˚C - 750˚C), carbonates (750˚C - 850˚C). Koro and Kaya clays can be heat-treated up to 400˚C without structural modification.

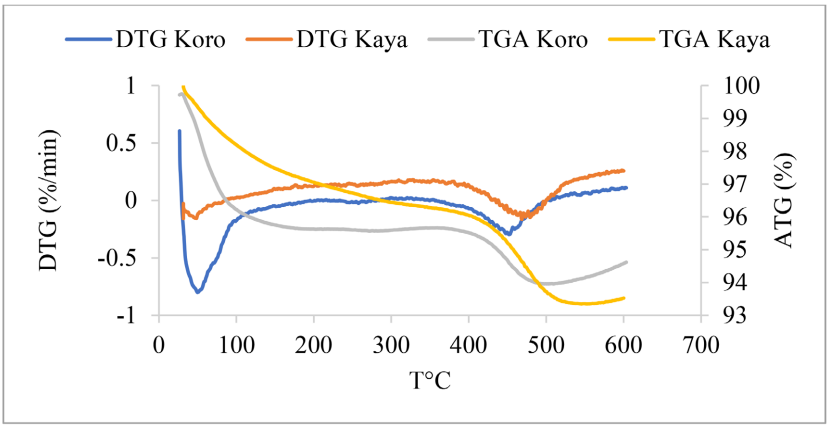

Figure 5. TGA/DTG curves of Koro and Kaya clays.

3.2. Chemical Composition

EDXRF results in Table 3 indicate a major silica and alumina content in both clays. The SiO_2/Al_2O_3 mass ratio was respectively 3.63 and 2.83 for Koro and Kaya, indicating the presence of free silica [32] with a composition rich in clay minerals [33]. Iron content was 6.76% and 3.44%, respectively for Koro and Kaya, indicating a low content of iron into the clays. According to [34], iron would be found in the form of hydroxide, which is probably responsible of brown color of Koro. Iron is a suitable element for cyanide removal through formation of strong Fe-CN bonds or stable complexes $Fe(CN)_6^{3-}$, $Fe(CN)_6^{4-}$ [34]. Both clays would contain very weak metals capable of stabilizing cyanide such as copper and zinc, which could lead to a release adsorbed cyanide.

Table 3. Chemical composition of Koro and Kaya (%, m/m).

Oxides (% wt)	SiO_2	Al_2O_3	Fe_2O_3	K_2O	CaO	Na_2O	MgO	TiO_2	ZnO	CuO	Total
Koro	53.00	24.60	6.76	3.42	1.21	1.33	1.31	0.80	0.01	0.01	92.45
Kaya	53.80	29.00	3.44	4.81	0.33	1.34	0.34	0.43	0.01	0.01	92.88

3.3. Mineral and Crystalline Phases

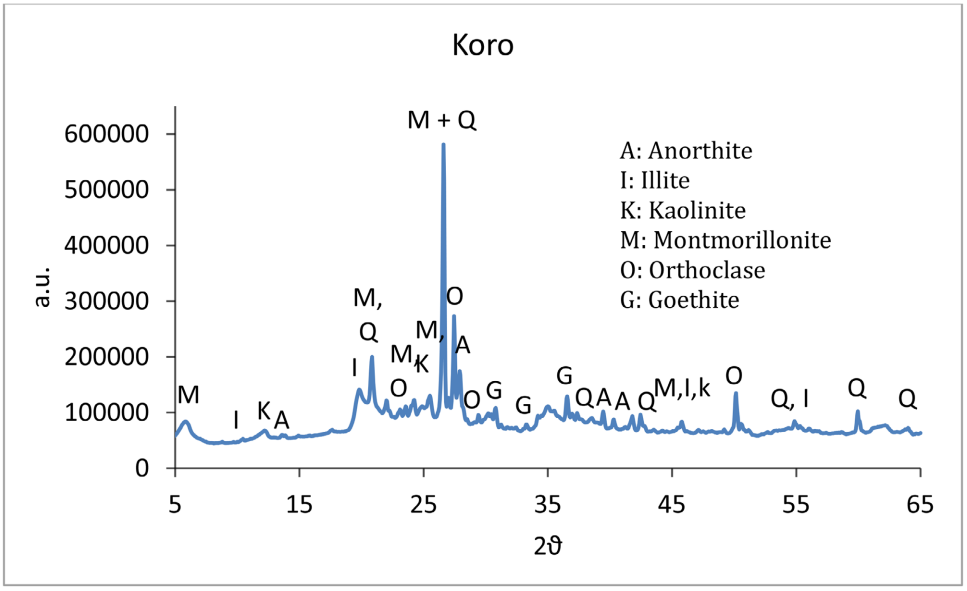

Figure 6. XRD diffractogram of Koro.

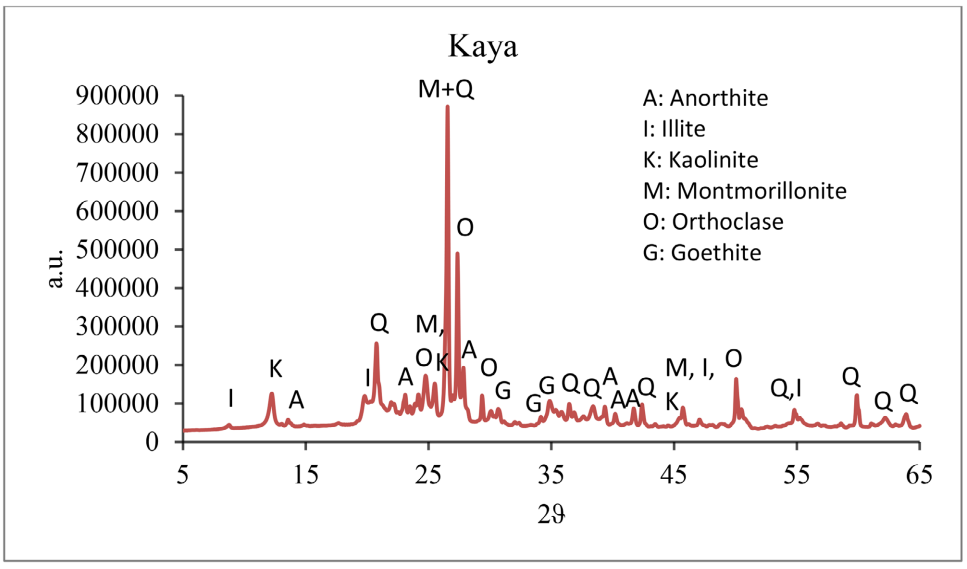

Figure 7. XRD diffractogram of Kaya.

Figure 6 and **Figure 7** show the X-ray diffraction patterns of Koro and Kaya, respectively. The XRD patterns revealed the presence of quartz (SiO_2), kaolinite

($Al_2Si_2O_5(OH)_4$), montmorillonite ($Al_{1.67}Mg_{0.33})Si_4O_{10}(OH)_2Na_{0.33}$), illite ((K, $H_3O)Al_2Si_3AlO_{10}(OH)_2$), orthosis ($KAlSi_3O_8$), anorthite ($CaAl_2Si_2O_8$) and goethite (FeO(OH)). Kaolinite and montmorillonite are minerals derived either from the alteration of primary minerals (peridots, pyroxenes, feldspars) or from the transformation of other secondary minerals such as illite and vermiculite [35]. Goethite in α-FeOOH form is the most abundant and stable of all forms of iron oxides in soil and its surface chemistry affects the distribution of soluble species in soil [36]. Results of XRD analysis of Koro are in agreement with those obtained by Sorgho *et al.* [37]. Quantitative content given in **Table 4**, showed that the clays contained mainly of illite, montmorillonite and kaolinite. Other phases such as quartz, anorthite, goethite and orthosis were moderately present. Previous studies have shown that montmorillonite [38], illite, and goethite [39] have a better potential in cyanide removal by adsorption. Minerals content of Koro and Kaya clays, make them good materials for cyanide removal from water.

Table 4. Mineralogical composition of Koro and Kaya clays.

	Kaolinite	Goethite	Orthose	Quartz	Montmorillonite	Illite	Anorthite
Koro	17.12	6.76	9.40	12.02	23.83	24.68	6.01
Kaya	26.28	3.44	13.22	4.91	24.01	27.49	1.63

3.4. Chemical Functions

Spectrum of Koro and Kaya (**Figure 8**) indicated the same chemical functions with slight differences in the intensity of absorption band. Based on previous studies, absorption peaks are attributed to chemical functions likely to be absorbed at its different positions. Adsorption bands of 1012 and 420 cm^{-1} are linked to the Si-O bond of kaolinite [40] [41], whereas those at 3697, 3624, and 522 cm^{-1} are related to the elongation vibration of the O-Al bond [42]. The -OH bond vibration of the water molecule is represented by the bands at 3380 and 1633 cm^{-1} [43]-[45]. The bands at 1012, 1004, 909, and 612 cm^{-1} are attributed to the vibration of the Fe-OH bond of goethite [46] [47]. The O-Al-Al band at 909 cm^{-1} and the Si-O-Al bands at 620 and 466 cm^{-1} can be used to identify montmorillonite [14] [41]. The vibration bands of elongation attributed to the Si-O bond at 1120, 744, 684, and 466 cm^{-1} indicate silica [32] [41]. Deformation vibrations of the AlOSi, AlMgOH and Al-Fe bonds in smectite are responsible for the 840 and 522 cm^{-1} bands [14] [48]. The bands at 520 and 460 cm^{-1} are attributable to the vibration of the Fe-O bond of the hematite [49]. The X-ray diffraction study showed the existence of goethite, quartz, montmorillonite, and kaolinite, but it did not report the presence of hematite or smectite. A low crystallinity or very low grade could be the cause of their lack in XRD. The intensity of the adsorption peaks of all functions increases when the spectra of the crude clays and the cyanide-adsorbing clays are compared (**Figure 9** and **Figure 10**). Physical adsorption or complexation with all elements would occur for cyanide.

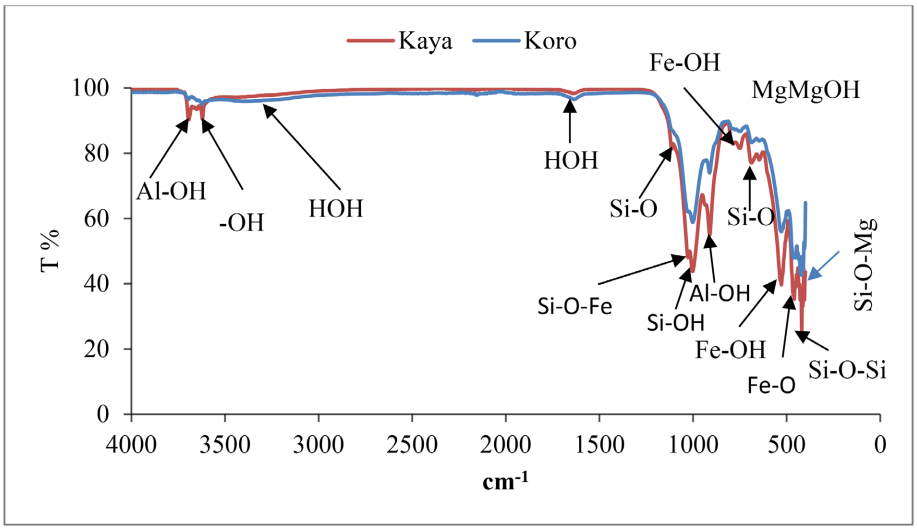

Figure 8. FT-IR spectra of Koro and Kaya.

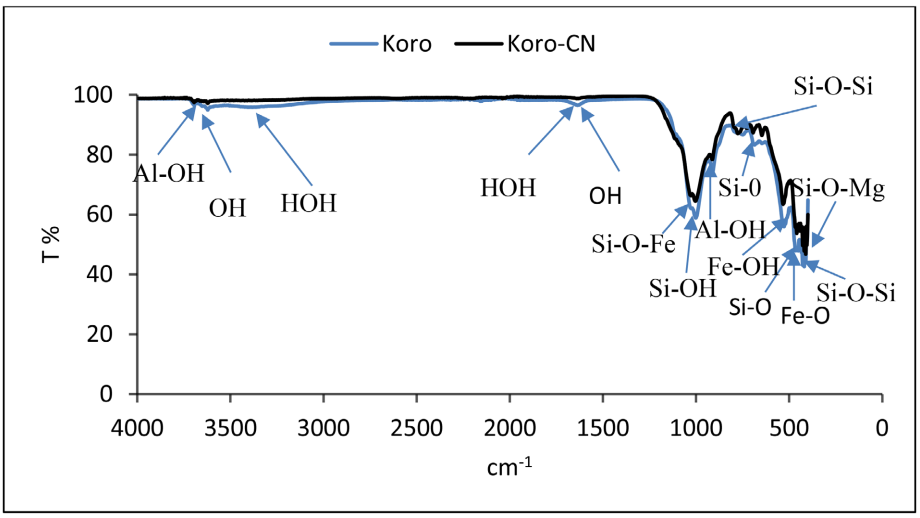

Figure 9. FT-IR spectra of adsorbed and raw Koro clay.

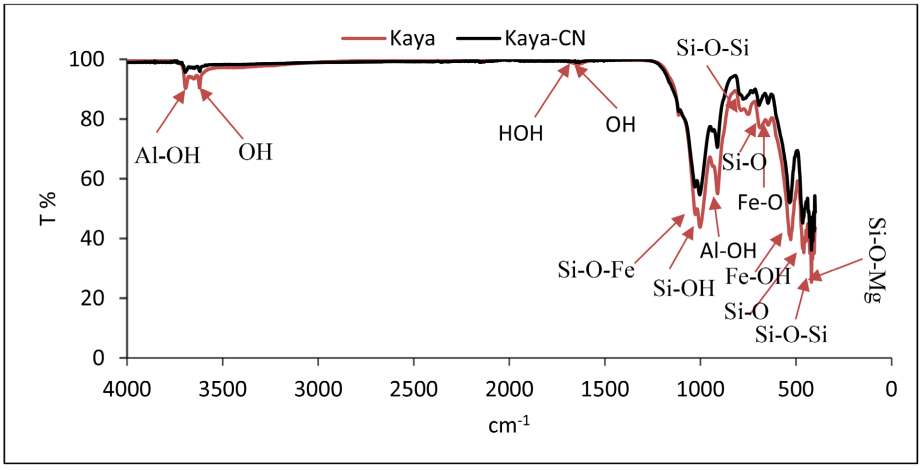

Figure 10. FT-IR spectra of adsorbed and raw Kaya clay.

3.5. Microstructure and Morphology of Clays

SEM images of Koro and Kaya (Figure 11 and Figure 12), respectively show the presence of macropores and reflective areas characteristic of heavy metals that can be attributed to iron. The absence perceptible of micropore could be justified by the small size of the grains which could limit the adsorption of cyanide by intra-molecular diffusion. There are deformed platelets, irregularly arranged, probably kaolinite. The presence of iron will promote cyanide removal through formation of strong Fe-CN bonds or stable complexes such as $Fe(CN)_6^{3-}$, $Fe(CN)_6^{4-}$ [34]. The surface of Kaya is in aggregate form, which could be linked to the presence of impurities and would justify its low value of specific surface compared to that of Koro [20].

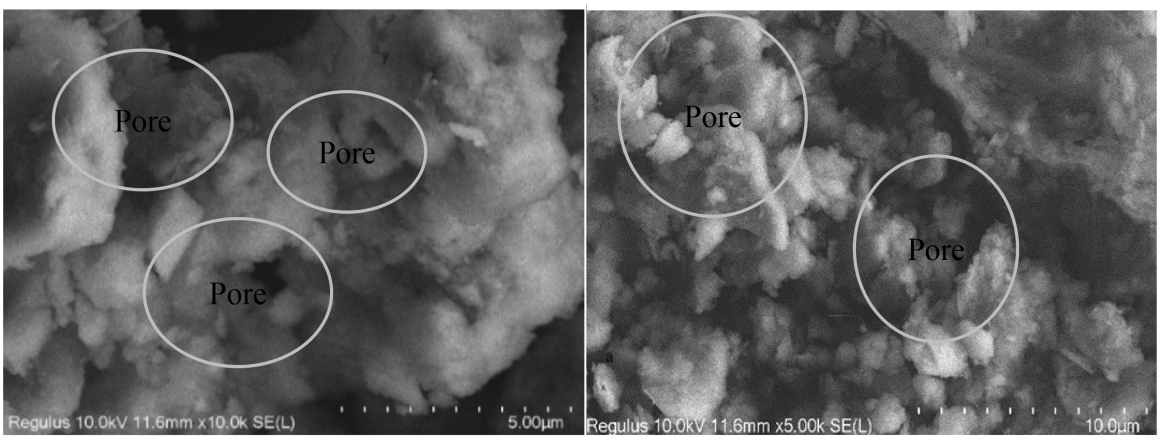

Figure 11. SEM images of Koro clay.

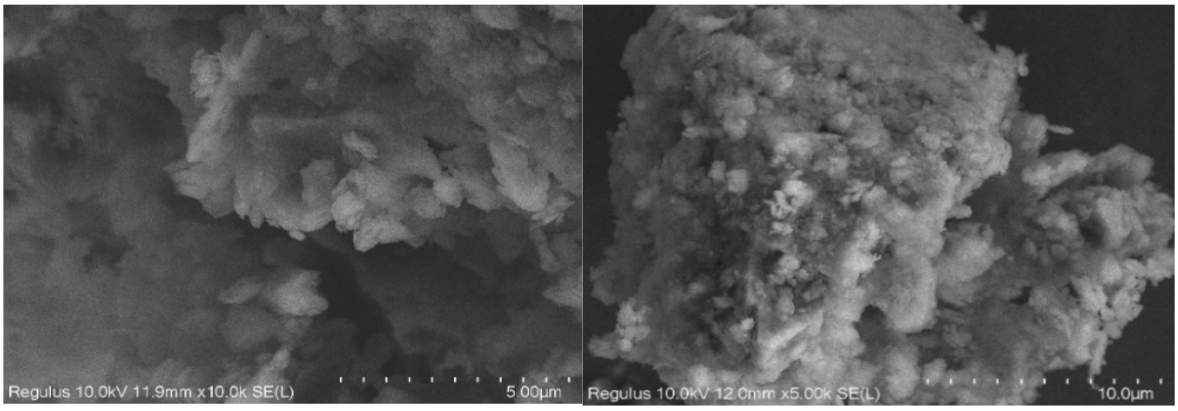

Figure 12. SEM images of Kaya clay.

Cliches analysis by the EDS detector allowed recording of EDS spectra (Figure 13). Qualitatively, the presence of aluminum (Al), silicon (Si), iron (Fe), oxygen (O) and carbon (C) was emerged. Quantitative analyses of these elements recorded in Table 5 show that they are mainly composed of O (56% - 61%), Si (15% - 18%), Al (4% - 6%) and weakly Fe (1% - 2%). Elements are in oxide or hydroxylated form [20], which is in agreement with FT-IR results.

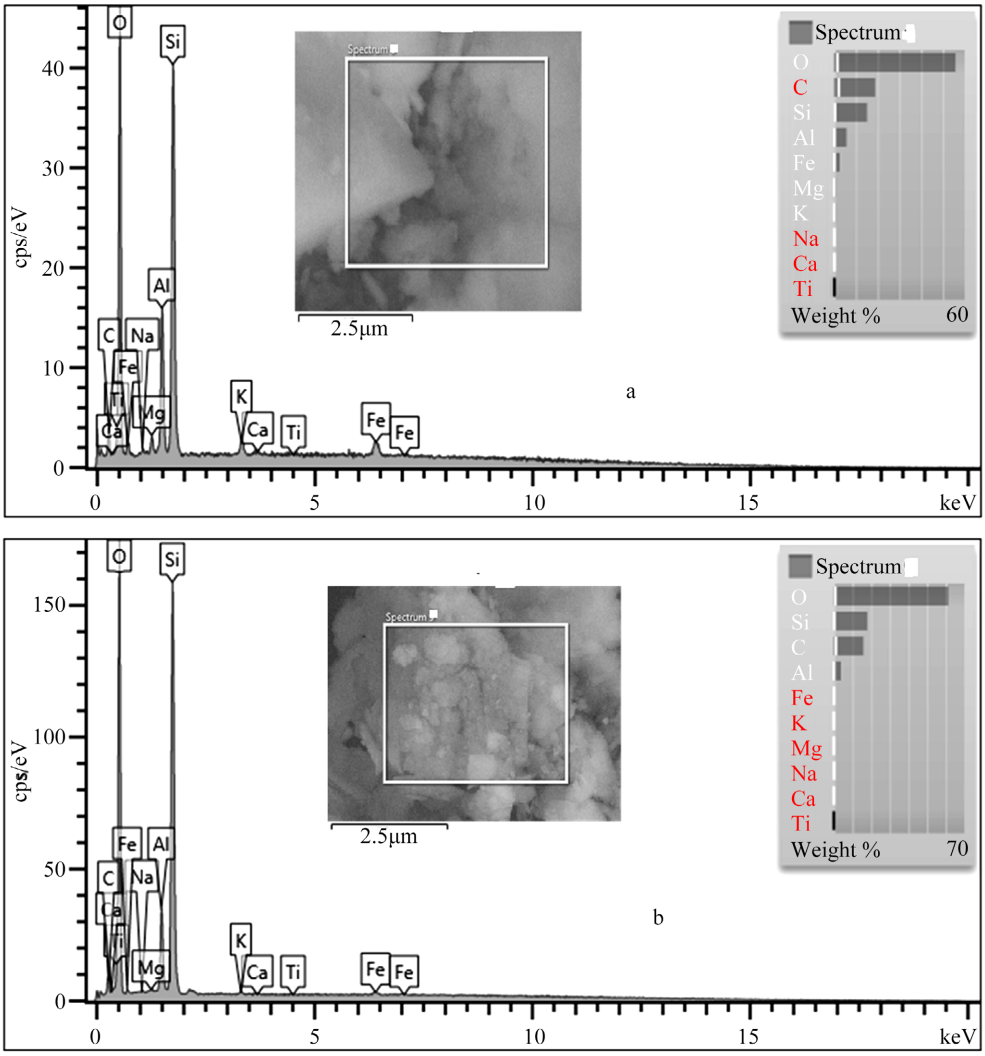

Figure 13. Energy dispersive spectroscopy spectra and SEM micrographs of snapshots of clays: (a) Koro; (b) Kaya.

Table 5. Elemental composition of Koro and Kaya.

Chemical element (% wt)	O	C	Si	Al	Fe	K	Ca	Mg	Na	Ti
Koro	55.75	18.86	15.11	5.68	2.49	0.84	0.11	0.90	0.23	0.04
Kaya	61.44	15.3	17.95	3.81	0.55	0.16	0.06	0.09	0.09	0.01

4. Conclusion

The use of clays as adsorbent deserved a good knowledge of their properties. Results of characterization showed two clays of different colors with higher iron content in Koro compared to Kaya. The two clays had very rich and similar mineralogical compositions. They contained mainly of illite, montmorillonite and kaolinite, moderately quartz, goethite, anorthite and orthose. Although Koro had the highest specific surface area, they both had the same anionic exchange capacity.

The mixing of clay and cyanide caused cyanide fixing, which was manifested as a change in surface morphology and an increase in chemical function intensities. It would be fascinating to look at the cyanide fixation process, the resulting processes, and the adsorption capacities.

Acknowledgements

The authors would like to thank the Laboratory of Faso for technical support and availability of work lab. TWAS and UNESCO are thankful for Individual Research Grant **Award_22-087 RG/CHE/AF/AC_I**, which enables us to carry out this study.

Authors' Contributions

RK is the main investigator of this work, he collected clays, carried out the work and wrote the manuscript. YS approved the methodology, oriented the work and corrected the manuscript. AC contributed to the characterization of clays and read the draft. RT and AK were involved in experiments and contributed to the writing of manuscript. SP is the scientific content of the manuscript by making the last corrections.

Conflicts of Interest

The authors declare no conflicts of interest regarding the publication of this paper.

References

[1] Ouedraogo, R., Nyantakyi, E.K., Sorgho, B., Siabi, E.K., Amproche, A.A., Obiri-Yeboah, A., *et al.* (2022) The Emergence of Artisanal Gold Mining and Local Perceptions in the Hounde Municipality, Burkina Faso. *Scientific African*, **17**, e01306. https://doi.org/10.1016/j.sciaf.2022.e01306

[2] Bohbot, J. (2017) L'orpaillage au Burkina Faso: Une aubaine économique pour les populations, aux conséquences sociales et environnementales mal maîtrisées. *EchoGéo*, **42**, 1-19. https://doi.org/10.4000/echogeo.15150

[3] Razanamahandry, L.C. (2017) Pollution environnementale par le cyanure et poten-tialités de la bioremédiation dans des zones d'extraction aurifère en Afrique Sub-Saharienne: Cas du Burkina Faso. Thèse Unique, Institut International d'Ingénierie de l'Eau et de l'Environnement, 223.

[4] Wang, P., Bai, Y., Yao, C., Li, X., Zhou, L., Wang, W., *et al.* (2017) Intracellular and *in Vivo* Cyanide Mapping via Surface Plasmon Spectroscopy of Single Au-Ag Nanoboxes. *Analytical Chemistry*, **89**, 2583-2591. https://doi.org/10.1021/acs.analchem.6b04860

[5] Malhotra, S., Pandit, M., Kapoor, J. and Tyagi, D. (2004) Photo-Oxidation of Cyanide in Aqueous Solution by the UV/H_2O_2 Process. *Journal of Chemical Technology & Biotechnology*, **80**, 13-19. https://doi.org/10.1002/jctb.1127

[6] Yadollahi, A. (2019) An Investigation on the Possibility of Cyanide Removal from the Industrial Wastewaters Using the Smectite Clay Minerals from the Mehrjan Area. *Journal of Mineral Resources Engineering*, **4**, 99-110. https://doi.org/10.30479/jmre.2019.9290.1167

[7] Mbadcam, J.K., Ngomo, H.M., Tcheka, C., Rahman, N., Djoyo, H.S. and Kouotou, D. (2009) Batch Equilibrium Adsorption of Cyanides from Aqueous Solution onto Copper- and Nickel-Impregnated Powder Activated Carbon and Clay. *Journal of*

Environmental Protection Science, **3**, 53-57.

[8] Halet, F., Yeddou, A.R., Chergui, A., Chergui, S., Nadjemi, B. and Ould-Dris, A. (2015) Removal of Cyanide from Aqueous Solutions by Adsorption on Activated Carbon Prepared from Lignocellulosic By-Products. *Journal of Dispersion Science and Technology*, **36**, 1736-1741. https://doi.org/10.1080/01932691.2015.1005311

[9] Dash, R.R., Balomajumder, C. and Kumar, A. (2009) Removal of Cyanide from Water and Wastewater Using Granular Activated Carbon. *Chemical Engineering Journal*, **146**, 408-413. https://doi.org/10.1016/j.cej.2008.06.021

[10] Manyuchi, M.M., Sukdeo, N. and Stinner, W. (2022) Potential to Remove Heavy Metals and Cyanide from Gold Mining Wastewater Using Biochar. *Physics and Chemistry of the Earth, Parts A/B/C*, **126**, Article ID: 103110. https://doi.org/10.1016/j.pce.2022.103110

[11] Peroxide, H., Khodadadi, A., Abdolahi, M. and Teimoury, P. (2005) Detoxification of Cyanide in Gold Processing Wastewater. *Journal of Environmental Health Science and Engineering*, **2**, 177-182.

[12] Young, C.A., Jordan, T.S. and Tech, M. (2011) Cyanide Remediation: Current and Technologies. Rapport of Department of Metallurgical Engineering (Montana), 104-129.

[13] Bergaya, F., Theng, B.K.G. and Lagaly, G. (2006) Handbook of Clay Science. Developments in Clay Science, Vol. 1, Elsevier, 1224.

[14] Madejová, J., Pálková, H. and Komadel, P. (2010) IR Spectroscopy of Clay Minerals and Clay Nanocomposites. In: Yarwood, J., *et al.*, Eds., *Spectroscopic Properties of Inorganic and Organometallic Compounds*, The Royal Society of Chemistry, 22-71. https://doi.org/10.1039/9781849730853-00022

[15] Sadik, C., El Amrani, I. and Albizane, A. (2012) Influence de la nature chimique et minéralogique des argiles et du processus de fabrication sur la qualité des carreaux céramiques. *MATEC Web of Conferences*, **2**, Article No. 01016. https://doi.org/10.1051/matecconf/20120201016

[16] Efeovbokhan, V.E., Olurotimi, O.O., Yusuf, E.O., Abatan, O.G. and Alagbe, E.E. (2019) Production of Clay Filters for Waste Water Treatment. *Journal of Physics: Conference Series*, **1378**, Article ID: 032028. https://doi.org/10.1088/1742-6596/1378/3/032028

[17] Combéré, W., Yonli, A.H. and Djandé, A. (2017) Elimination du chrome trivalent des eaux par des zéolithes échangées au fer et des argiles naturelles du Burkina Faso. *Journal de La Société Ouest-Africaine de Chimie*, **43**, 26-30.

[18] Brahima, S., Samuel, P., Boubié, G., Lamine, Z., Karfa, T. and Ingmar, P. (2011) Etude d'une argile locale du Burkina Faso à des fins de décontamination en Cu^{2+}, Pb^{2+} et Cr^{3+}. *Journal de la Société Ouest-Africaine de Chimie*, **31**, 49-59.

[19] Fernandez, R., Martirena, F. and Scrivener, K.L. (2011) The Origin of the Pozzolanic Activity of Calcined Clay Minerals: A Comparison between Kaolinite, Illite and Montmorillonite. *Cement and Concrete Research*, **41**, 113-122. https://doi.org/10.1016/j.cemconres.2010.09.013

[20] Qlihaa, A., Dhimni, S., Melrhaka, F., Hajjaji, N. and Srhiri, A. (2016) Caractérisation physico-chimique d'une argile Marocaine. *Journal of Materials and Environmental Science*, **7**, 1741-1750.

[21] Errais, E. (2011) Réactivité de surface d'argiles naturelles Etude de l'adsorption de colorants anioniques. Thèse Unique, Géochimie de l'Environnement, Université de Strasbourg.

[22] Pansu, M. and Gautheyrou, J. (2006) Anion Exchange Capacity. Springer. https://doi.org/10.1007/978-3-540-31211-6_27

[23] Laibi, A.B., Gomina, M., Sorgho, B., Sagbo, E., Blanchart, P., Boutouil, M., *et al.* (2017) Caractérisation physico-chimique et géotechnique de deux sites argileux du Bénin en vue de leur valorisation dans l'éco-construction. *International Journal of Biological and Chemical Sciences*, **11**, 499-514. https://doi.org/10.4314/ijbcs.v11i1.40

[24] Ouedraogo, R.D., Bakouan, C., Sorgho, B., Guel, B. and Bonou, L.D. (2020) Caractérisation d'une latérite naturelle du Burkina Faso en vue de l'élimination de l'arsenic (III) et l'arsenic (V) dans les eaux souterraines. *International Journal of Biological and Chemical Sciences*, **13**, 2959-2977. https://doi.org/10.4314/ijbcs.v13i6.41

[25] Kaboré, R., Yacouba Sanou, Konaté, A. and Paré, S. (2024) Study of the Efficiency of Two Clays Soils for Cyanide Removal in Water: Kinetic and Equilibrium Modelling. *Asian Journal of Physical and Chemical Sciences*, **12**, 1-14. https://doi.org/10.9734/ajopacs/2024/v12i2220

[26] Fies, J., Stengel, P., Bourlet, M., Horoyan, J. and Jeandet, C. (1981) Densité texturale de sols naturels II. Eléments d'interprétation. *Agronomie*, **1**, 659-666. https://doi.org/10.1051/agro:19810807

[27] Abebe, B., Murthy, H.C.A. and Amare, E. (2018) Summary on Adsorption and Photocatalysis for Pollutant Remediation: Mini Review. *Journal of Encapsulation and Adsorption Sciences*, **8**, 225-255. https://doi.org/10.4236/jeas.2018.84012

[28] Önal, Y., Akmil-Başar, C. and Sarıcı-Özdemir, Ç. (2007) Investigation Kinetics Mechanisms of Adsorption Malachite Green onto Activated Carbon. *Journal of Hazardous Materials*, **146**, 194-203. https://doi.org/10.1016/j.jhazmat.2006.12.006

[29] Diatta, M.T. (2016) Matières premières argileuses du Sénégal: Caractéristiques et applications aux produits céramiques de grande diffusion Thèse en Cotutelle, Matériaux, Université de Limoges, 158.

[30] Lamine, S.M. (2013) Étude des propriétés adsorbantes des charbons activés issus des noyaux de dattes. Application au traitement d'effluent aqueux. Thèse Unique, Génie Chimique, Université Badji Mokhtar-Annaba (Algérie), 98.

[31] Sedjro, Y., Kiki, T., Sedjro, Y. and Kiki, T. (2017) Caractérisation minéralogique, thermique et microscopique des sols fins en technique routière. Thèse Unique, Science de l'Ingénieur, Université de Bordeaux, 211.

[32] Zerbo, L. (2009) Transformations thermiques et reorganisation structurale d'une argile du Burkina Faso. Thèse Unique, Chimie, Université Joseph Ki-Zerbo, 163.

[33] Abdoulkader, M., Malam Salmanou Souleymane, I., Bouba, H., Toure Amadou, A., Zibo, G. and Ibrahim, W. (2021) Caractérisation Physico-Chimique et Minéralogique des Argiles De La Carrière De Mirriah, Région De Zinder, Utilisées Dans La Poterie. *European Scientific Journal, ESJ*, **17**, 120-132. https://doi.org/10.19044/esj.2021.v17n3p120

[34] Botz, M.M., Mudder, T.I. and Akcil, A.U. (2016) Cyanide Treatment: Physical, Chemical, and Biological Processes. In: Adams, M.D., Ed., *Gold Ore Processing: Project Development and Operations*, Elsevier, 619-645. https://doi.org/10.1016/b978-0-444-63658-4.00035-9

[35] Tertre, E. (2005) Adsorption de Cs^{+}, Ni^{2+} et des lanthanides sur une kaolinite et une smectite jusqu'à 150˚C: Étude expérimentale et modélisation. Thèse Unique, Géochimie, Université Toulouse III.

[36] Jaiswal, A., Banerjee, S., Mani, R. and Chattopadhyaya, M.C. (2013) Synthesis, Characterization and Application of Goethite Mineral as an Adsorbent. *Journal of Environmental Chemical Engineering*, **1**, 281-289. https://doi.org/10.1016/j.jece.2013.05.007

[37] Sorgho, B., Bressollier, P., Guel, B., Zerbo, L., Ouedraogo, R., Gomina, M., *et al.* (2016)

Étude des propriétés mécaniques des géomateriaux argileux associant la décoction de Parkia Biglobosa (néré). *Comptes Rendus. Chimie*, **19**, 895-901. https://doi.org/10.1016/j.crci.2016.01.016

[38] Colin-Garcia, M., Heredia, A., Negron-Mendoza, A., Ortega, F., Pi, T. and Ramos-Bernal, S. (2014) Adsorption of HCN onto Sodium Montmorillonite Dependent on the Ph as a Component to Chemical Evolution. *International Journal of Astrobiology*, **13**, 310-318. https://doi.org/10.1017/s1473550414000111

[39] Rennert, T., Kaufhold, S. and Mansfeldt, T. (2005) Sorption of Iron-Cyanide Complexes on Goethite Investigated in Long-Term Experiments. *Journal of Plant Nutrition and Soil Science*, **168**, 233-237. https://doi.org/10.1002/jpln.200421602

[40] Joussein, E., Petit, S. and Decarreau, A. (2001) Une nouvelle méthode de dosage des minéraux argileux en mélange par spectroscopie IR. *Comptes Rendus de l'Académie des Sciences—Series IIA—Earth and Planetary Science*, **332**, 83-89. https://doi.org/10.1016/s1251-8050(01)01511-7

[41] Ritz, M., Vaculíková, L. and Plevová, E. (2010) Identification of Clay Minerals by Infrared Spectroscopy and Discriminant Analysis. *Applied Spectroscopy*, **64**, 1379-1387. https://doi.org/10.1366/000370210793561592

[42] Bakouan, C. (2018). Caractérisation de quelques sites latéritiques du Burkina Faso: Application à l'élimination de l'arsenic (III) et (V) dans les eaux souterraines. Thèse Unique, Chimie Université Joseph Ki-Zerbo, 241.

[43] Sdiri, A.T., Higashi, T. and Jamoussi, F. (2013) Adsorption of Copper and Zinc onto Natural Clay in Single and Binary Systems. *International Journal of Environmental Science and Technology*, **11**, 1081-1092. https://doi.org/10.1007/s13762-013-0305-1

[44] Blanchard, M., Balan, E., Giura, P., Béneut, K., Yi, H., Morin, G., *et al.* (2013) Infrared Spectroscopic Properties of Goethite: Anharmonic Broadening, Long-Range Electrostatic Effects and Al Substitution. *Physics and Chemistry of Minerals*, **41**, 289-302. https://doi.org/10.1007/s00269-013-0648-7

[45] Tomić, Z., Makreski, P. and Gajić, B. (2009) Identification and Spectra-Structure Determination of Soil Minerals: Raman Study Supported by IR Spectroscopy and X-Ray Powder Diffraction. *Journal of Raman Spectroscopy*, **41**, 582-586. https://doi.org/10.1002/jrs.2476

[46] Chatterjee, S. and De, S. (2015) Application of Novel, Low-Cost, Laterite-Based Adsorbent for Removal of Lead from Water: Equilibrium, Kinetic and Thermodynamic Studies. *Journal of Environmental Science and Health, Part A*, **51**, 193-203. https://doi.org/10.1080/10934529.2015.1094321

[47] Lakshmipathiraj, P., Narasimhan, B.R.V., Prabhakar, S. and Bhaskar Raju, G. (2006) Adsorption Studies of Arsenic on Mn-Substituted Iron Oxyhydroxide. *Journal of Colloid and Interface Science*, **304**, 317-322. https://doi.org/10.1016/j.jcis.2006.09.024

[48] Kuligiewicz, A., Derkowski, A., Szczerba, M., Gionis, V. and Chryssikos, G.D. (2015) Revisiting the Infrared Spectrum of the Water—Smectite Interface. *Clays and Clay Minerals*, **63**, 15-29. https://doi.org/10.1346/ccmn.2015.0630102

[49] Laversin, H. (2013) Technique de préparation des minéraux argileux en vue de l'analyse par diffraction des Rayons X et introduction à l'interprétation des diagrammes. Thèse Unique Chimie, Université du Litto, 175.